Eur Biophys J (1994) 23:115–123

European Biophysics Journal

Vibrational analysis and molecular force field of hypoxanthine as determined from ultraviolet resonance Raman spectra of native and deuterated species

J. Ulicny [1], M. Ghomi [2], A. Tomkova [1], P. Miskovsky [1], P. Y. Turpin [3], L. Chinsky [3]

[1] Department of Biophysics, Safarik University, 04154 Kosice, Slovakia
[2] Physique Théorique des Macromolécules Biologiques, UFR Santé-Médecine-Biologie Humaine, Université Paris XIII, 74 rue Marcel Cachin, F-93012 Bobigny Cedex, France
[3] Laboratoire de Physique et Chimie Biomoléculaires, CNRS URA 198, Institut Curie et Université Paris VI, 11 rue Pierre et Marie Curie, F-75231 Paris Cedex 05, France

Received: 29 September 1993 / Accepted in revised form: 28 February 1994

Abstract. Ultraviolet resonance Raman scattering spectra from aqueous solutions of hypoxanthine and its deuterated species (C8-deuterated, N-deuterated and C8-, N-deuterated derivatives) have been collected and reported in the spectral region between 400 and 1800 cm^{-1}. The laser excitation wavelengths at 281 nm and 257 nm correspond to preresonance and pure resonance conditions, respectively, with the purine strongly allowed $\pi \rightarrow \pi^*$ electronic transition: thus the observed experimental Raman features mainly correspond to in-plane vibrational modes. The latter were then assigned according to the Wilson GF method by using an empirical harmonic valence force field. Normal mode calculations are based on a non-redundant set of internal coordinates. The calculated vibrational mode wavenumbers and their isotopic shifts upon selective deuterations are in good agreement with the experimental data. The present normal mode analysis rests on the transferability of the guanine and adenine force constants proposed in recent works based on resonance Raman spectroscopy and neutron inelastic scattering data from these major purine bases.

Key words: Resonance Raman spectroscopy – Vibrational analysis – Hypoxanthine – Nucleic acids – Molecular force field

I. Introduction

Hypoxanthine is one of the minor purine bases which forms only two hydrogen bonds with its complementary molecule in RNA/DNA double helical chains in which it participates. This is due to the lack of the amino group at the C2 position, as compared to the guanine molecule: these changes in the molecular structure and H-bond network are not without consequence for the stability and conformational transitions of double helical chains involving inosine residues, such as poly(dI-dC). This has been proved by numerous studies of poly(dI-dC): X-ray of low humidity fibers (Mitsui et al. 1970), CD (Vorlickova and Sagi 1991), vacuum CD (Sutherland and Griffin 1983), 2D NMR (Mirau and Kearns 1984), Raman (Weidlich et al. 1990) and UV resonance Raman (RRS) (Miskovsky et al. 1993) spectroscopies.

However, although off-resonance Raman spectra of inosine (rI) and 5′-IMP in aqueous solutions have been previously published (Medeiros and Thomas 1971), no experimental result yet exists on the proper hypoxanthine base in aqueous solution, probably because of the very poor water solubility of the base. Thus, the present UV RRS study aims to determine the vibrational modes of this base and to properly assign them, with the prospect of understanding the changes of the inosine conformational vibrational markers observed during structural transitions of nucleic acids in which inosine is involved.

In this regard, one can rely on previous results dealing with the major purine bases (guanine and adenine) and their deuterated species, obtained from RRS spectra of aqueous solutions and neutron inelastic scattering (NIS) data for polycrystalline samples (Coulombeau et al. 1991; Dhaouadi et al. 1993a, 1993b). A normal mode analysis of G and A, based on an empirical harmonic valence force field, allowed RRS and NIS vibrational mode wavenumbers and intensities to be simulated. We transferred these force fields previously calculated to the case of modified or minor bases: off- and on-resonance Raman spectra from aqueous solutions of 2-aminoadenine and its deuterated species have been recently successfully assigned and reported (Dhaouadi et al. 1994). In the present work, we report preresonance (281 nm) and RRS (257 nm) spectra of hypoxanthine and its deuterated derivatives, and in the same manner as for 2-aminoadenine, we propose an empirical harmonic valence force field allowing the in-plane vibrational motions to be assigned.

Correspondence to: M. Ghomi

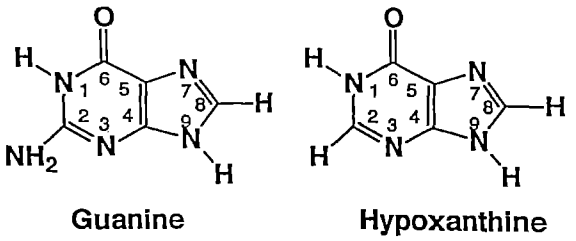

Fig. 1. Chemical structure and atom numbering of the guanine and hypoxanthine molecules

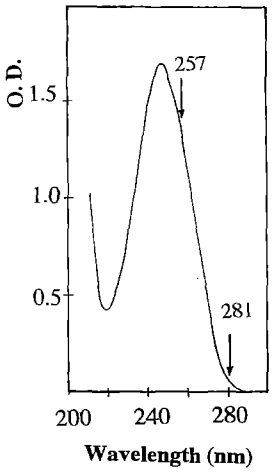

Fig. 2. Ultraviolet electronic absorption spectrum of hypoxanthine. The positions of the two ultraviolet excitation wavelengths used for recording RRS spectra, are indicated by vertical arrows

II. Methods and experimental results

Hypoxanthine base was purchased from Sigma and used as supplied. Hypoxanthine chemical structure and atom numbering are compared to those of guanine in Fig. 1. The C8-deuterium substitution was achieved by heating a hypoxanthine D_2O solution for three hours at 80 °C (Livramento and Thomas Jr. 1974, Thomas Jr. and Livramento 1975), and recrystallization from D_2O. Then, this species was dissolved in D_2O phosphate buffer, pD 7, to obtain the so-called H-d3 species (C8-, N1-, N9-deuterated hypoxanthine), or in a H_2O phosphate buffer for the so-called H-d1 species (C8-deuterated hypoxanthine) before Raman measurements. The H-d2 (N1-, N9-deuterated hypoxanthine) species was prepared by merely dissolving hypoxanthine base in a D_2O phosphate buffer at pD 7.

As stated above, hypoxanthine water solubility is very poor at room temperature: for this reason its Raman spectrum has never been obtained in aqueous solution. Nevertheless, its solubility is sufficient to obtain 257 nm resonance Raman spectra of good quality in a 10^{-2} M phosphate buffer, pH 7 (pD 7). Indeed the 257 nm excitation wavelength corresponds to almost optimum resonance conditions for the molecule: this is shown on the electronic absorption spectrum of hypoxanthine taken in aqueous solution (Fig. 2, recorded at room temperature on a VARIAN DMS 70 UV-visible spectrometer), which

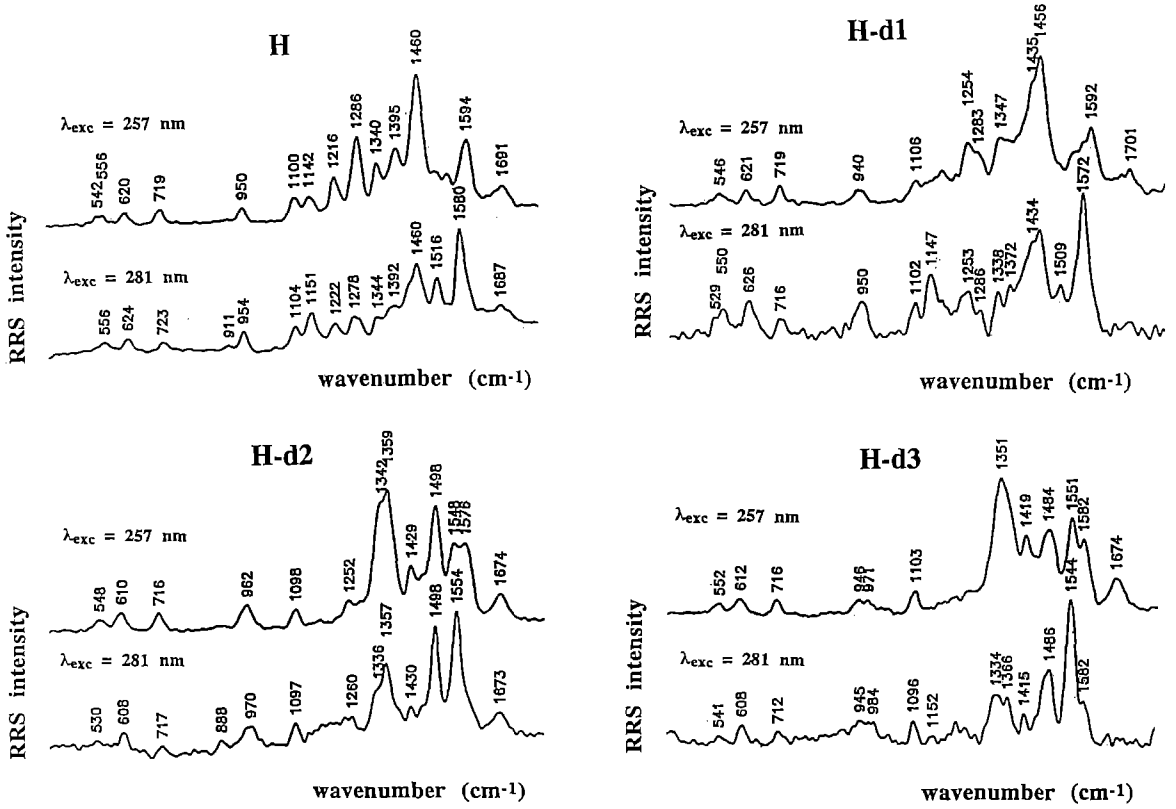

Fig. 3. Room temperature RRS spectra from aqueous solutions of hypoxanthine and its deuterated species in the 1800–400 cm^{-1} spectral region. Excitation wavelengths λ_{exc} = 257 and 281 nm are reported at the left of each spectrum. H: hypoxanthine; H-d1: C8-deuterated derivative of hypoxanthine; H-d2: N1-, N9-deuterated derivative of hypoxanthine; H-d3: C8-, N1-, N9-deuterated of hypoxanthine

Table 1. Non diagonal (interaction) valence force constants for hypoxanthine (H) and its deuterated species. These force constants are compared to those of guanine (G) and adenine (A) (Dhaouadi et al. 1993a, 1993b). Diagonal force constants (not shown here) are those used in our previous calculations on adenine and guanine bases (Dhaouadi et al. 1993a, 1993b, see also the text)

Interactions	Values	Interactions	Values
Stretch–Stretch		Stretch–Bend	
N9C8, N9C4	0.990 (0.990 G)	C6=O, adj. bend.	0.900 (0.900 G)
C=O, ν(py)	0.790 (0.600 G)	C8N9, CN9H	0.250 (0.100 G)
N1C6, adj. str.	0.545 (0.750 G)	N3C4, C4N3C2	0.210 (0.990 G)
N9C8, C8N7	0.900 (0.900 G)	N3C4, N3C4C5	0.350 (0.990 G)
N7C5, C8N7	0.690 (0.690 G)	N9C8, C4N9C8	−0.310 (−0.300 G)
N7C5, C4C5	0.820 (0.680 G)	N9C8, N7C8N9	−0.280 (−0.300 G)
C4C5, C4N9	0.750 (0.550 G)	C5C6, C5C6=O	−0.415 (0.300 G)
C2N3, C2N1	0.100 (0.990 G)	N1C6, N1C6=O	−0.150 (0.500 G)
C2N3, N3C4	0.000 (0.990 G)	C8N9, N9C8H	0.460 (0.990 G)
C5C4, N3C4	0.850 (0.850 G)	C8N7, N7C8H	0.200 (0.450 G)
C5C4, C5C6	0.850 (0.850 G)	C6N1, C6N1H	−0.100 (−0.070 G)
C5C4, C2N3	0.800 (0.600 G)	C8N7, C8N7C5	−0.700 (−0.600 G)
C5C4, C8N7	0.000 (−0.100 G)	C5N7, adj. bend	0.515 (−0.050 G)
		C4-N9, C4N9C8	0.000 (0.670 G)
		C8N7, N9C8N7	−0.600 (−0.600 G)
Bend–Bend		C4C5, N9C4C5	0.750 (0.450 G)
		C4C5, N7C5C4	1.070 (0.450 G)
C4N9H, C4N9C8	0.205 (0.450 G)	N1C2, N3C2N1	0.380 (0.970 G)
C8N9H, C4N9C8	0.450 (0.450 G)	N1C2, C2N1C6	0.475 (0.970 G)
C6N1H, C6N1C2	−0.350 (0.100 G)	C2N3, C4N3C2	0.300 (0.990 G)
C2N1H, C6N1C2	0.000 (0.100 G)	C2N3, N3C2N1	−0.255 (0.990 G)
N7C8H, N9C8N7	−0.200 (0.000 G)	C6N1, C2N1C6	0.735 (0.990 G)
N9C8H, N9C8N7	0.000 (0.000 G)	C6N1, N1C6C5	0.405 (0.990 G)
N3C2N1, NC2H	−0.430 (0.000 G)	C5C6, C4C5C6	0.990 (0.990 G)
		C5C6, N1C6C5	1.045 (0.990 G)
		C5C4, C6C5C4	0.350 (0.350 G)
		C5C4, C5C4N3	0.350 (0.350 G)
		N1C2, C2N1H	0.300 (0.000 G)
		C4N9, C4N9H	0.295 (0.000 G)
		C4N9, C8N7C5	0.485 (0.000 G)
		C4N9, N9C4C5	0.900 (0.670 G)
		C2N1, N1C2H	0.900 (0.000 A)
		C2N3, N3C2H	0.400 (0.000 A)

Units: Stretch–Stretch force constants (mdyn.Å), Bend–Bend force constants (mdyn.Å), Stretch–Bend force constants (mdyn). For atom numbering, see Fig. 1

yields an intense band peaking at 247 nm. However, 281 nm gives rise only to a preresonance Raman effect, and consequently the quality of the 281 nm spectra obtained from the same solution was poorer than that of the 257 nm spectra. We chose not to increase the solubility by heating the solutions, since in that case there would be some chance of reverse C8 deuterium-hydrogen exchange for H-d1 sample in H_2O solution, and conversely of partial C8 hydrogen-deuterium exchange for H-d2 sample in D_2O solution. Consequently, although the 257 and 281nm spectra are not of consistent quality, we collected them all in the 400–1800 cm^{-1} region by using the upper concentration limit (in H_2O and D_2O) which can be reached at room temperature (Fig. 3).

The experimental setup for RRS measurements has been described elsewhere (Miskovsky et al. 1989). The spectra displayed in Fig. 3 are the results of 5 to 8 successive accumulation scans, with a spectral resolution of ± 2 cm^{-1}. It has been necessary to subtract from all spectra the appropriate buffer contribution in the broad O–H (O–D) bending region around 1640 (1250) cm^{-1}, by taking as intensity standard the large O–H (O–D) stretching bands located in the 3450 (2500) cm^{-1} region.

III. Normal mode analysis

The vibrational mode wavenumbers and the atomic displacements were computed by using a home-made calculation code (BORNS) developed with the framework of the Wilson GF-method (Wilson et al. 1955). The redundant internal coordinates were removed by a diagonalization procedure of the *G*-matrix (Gusoni and Zerbi 1968).

Hypoxanthine base (Fig. 1) and its deuterated species H-d1, H-d2, and H-d3 are supposed to be planar (C_s symmetry). Thus, 36 vibrational modes can be expected from these molecules, among which 25 are in-plane (A′-symmetry) and 11 out-of-plane (A″-symmetry). Only the in-plane modes have been considered in the present calculations. In addition, only 21 calculated ring modes have been reported in the current paper and compared with the preresonance and RRS data, since the four N–H and

C–H (N–D and C–D) stretching modes are not active in preresonance and RRS.

A complete analysis of guanine vibrational modes, based on RRS and NIS spectra, by means of an empirical harmonic internal valence force field had been recently reported (Dhaouadi et al. 1993 b). The principal (diagonal) force constants were taken from Majoube (1984). Owing to the structural similarity between guanine and hypoxanthine (Fig. 1), the diagonal force constants of guanine have been transferred to hypoxanthine (Table 1). The diagonal force constants defined around the C2-position have been simply transferred from adenine (Dhaouadi et al. 1993 a). In order to simulate 67 experimental wavenumbers observed in the RRS spectra of hypoxanthine and its deuterated species, it has been necessary to refine only 41 off-diagonal force constants (out of 53) by a least squares method: only the force constants providing the most important Jacobian matrix values (for pure and deuterated species) were selected and refined. The interaction force constants of hypoxanthine, which have been adopted here, are listed in Table 1, which also shows the values of the guanine interaction force constants for comparison.

As in the case of guanine and adenine (Dhaouadi et al. 1993 a, b) some of the interaction force constant values are close to one (8 out of 63 are greather than 0.85): this does not seem unreasonable since these values remain markedly weaker than most of the diagonal bending force constants (and far weaker than the diagonal stretching force constants, which generally exceed several units). From our previous experience, this refinement procedure of the off-diagonal force constants only is the least perturbing means for fitting the calculated and observed frequencies and for simulating the isotopic shifts. Attempts made in varying the diagonal force constants, even in significant proportions, were much less efficient an led to changes of only a few wavenumbers in the vibrational modes, far too weak to correctly assign the actual observed wavenumbers of hypoxanthine and their isotopic shifts. In addition, it is not surprising that the largest difference between guanine and hypoxanthine off-diagonal force constants are those involving the C2 position, i.e. the site of chemical structure modification.

The calculated wavenumbers of the in-plane modes, as well as their assignments based on the Potential Energy Distribution (PED) matrix, are reported in Tables 2 to 5 for hypoxanthine, H-d1, H-d2 and H-d3 species, respectively. Only PED values equal to or greater than 7% are reported (except for a few modes in which the vibrational PED is largely distributed over the whole molecule). Tables 2 to 5 also show the experimental RRS peak positions obtained for both 257 and 281 nm excitation wavelengths (according to Fig. 3).

The graphical representation of hypoxanthine atomic displacements are presented in Fig. 4. This is of greater interest in understanding the origin and the nature of the vibrational modes and the correspondence existing between them. To represent graphically a vibrational mode, the equilibrium structure as well as the most distorted configurations have been drawn on the same figure.

IV. Discussion

21 vibrational modes have been calculated in the spectral region below 1750 cm^{-1} for hypoxanthine and its deuterated species (Tables 2–5). On the basis of these assign-

Table 2. Comparison between experimental and calculated wavenumbers (cm^{-1}) for hypoxanthine in-plane modes, in the spectral region below 1800 cm^{-1}. The assignments are based on the internal coordinates for which the potential energy distribution (PED) is reported in % (PED contributions lower then 7% are not reported). The experimental wavenumbers from aqueous solution Raman spectra at two UV excitation wavelengths (present work, see also Fig. 3) are also reported. (vs): very strong, (s): strong, (m): middle, (w): weak, (vw): very weak, (sh): shoulder, (b): broad

RRS 257 nm	RRS 281 nm	Calc.	Assignments (PED)
1691 (m, br)	1687 (w)	1720	C6=O (43%), C6-N1 (7%)
		1682	N3-C4 (28%), C2=N3 (19%), C6=O (12%), C5-C6 (9%)
1594 (s)	1590 (sh)	1606	C8=N7 (42%)
	1580 (s)	1573	C5-C6 (34%), N7-C5 (18%), C6-N1 (9%), C2=N3 (8%)
	1516 (m)	1531	C4-N3=C2 (13%), C2=N3 (11%); N1-C2 (10%), N3-C4-N9 (9%), C8=N7 (8%)
1460 (s)	1460 (s)	1462	N1-C2-H (22%), N3=C2-H (11%), C5=C4 (11%), C2=N3 (8%)
	1439 (m, sh)	1446	C4-N9 (26%), N9-C8 (17%)
1395 (m)	1392 (w)	1397	C2=N3 (18%), N9-C8 (16%), N1-C2 (12%), N3-C4 (12%)
1340 (m)	1344 (w)	1324	N3=C2-H (35%); N1-C2-H (25%), C5=C4 (8%)
1286 (s)	1286 (w)	1282	N7=C8-H (25%), H-N9-C8 (20%), N9-C8-H (18%), H-N9-C4 (17%)
	1278 (w)	1257	C6-N1-H (39%), C2-N1-H (26%), C6=O (17%)
1216 (m)	1222 (w)	1208	N9-C8-H (21%), H-N9-C8 (21%), N7=C8-H (20%), H-N9-C4 (15%), N9-C8 (11%)
1142 (m)	1151 (m)	1148	C6-N1 (26%), N7-C5 (19%), N9-C8-H (9%), N7=C8-H (9%), N1-C2 (8%)
1100 (m)	1104 (m)	1089	C6=O (15%), N1-C2 (14%), N3-C4 (10%), N9-C8 (9%)
950 (m)	954 (m)	929	N1-C2 (23%), C2=N3 (10%), N7-C5 (8%), C4-N9 (8%)
	911 (vw)	899	N9-C8=N7 (17%), N9-C8-H (11%), N9-C8 (11%), C8=N7-C5 (11%), C4-N9-C8 (11%), H-N9-C4 (9%)
719 (m)	723 (w)	694	N3-C4 (11%), N1-C2 (9%); N1-C6-C5 (8%)
620 (w)	624 (w)	618	C6-N1 (12%), C8=N7-C5 (9%), N7-C5=C4 (9%), C4-N9 (8%)
556 (vw)	556 (vw)	569	N7-C5 (21%), C6-N1 (17%), N7-C5-C6 (10%), C6-C5=C4 (9%), C5-C6=O (8%)
542 (vw)		522	N3-C4 (17%), N3-C4-N9 (14%), C4-N9 (14%), N1-C6=O (11%)
		313	C5-C6 (26%), C5-C6=O (25%), N1-C6=O (19%)

Table 3. Same as Table 2, but for H-d1 (C8-deuterated derivative of hypoxanthine). See also Fig. 3

RRS 257 nm	RRS 281 nm	Calc.	Assignments (PED)
		1719	C6=O (44%),C6-N1 (8%)
1701 (w)		1682	N3-C4 (28%), C2=N3 (19%), C6=O (12%), C5-C6 (9%)
1592 (s)	1590 (sh)	1594	C8=N7 (36%)
1572 (sh)	1572 (vs)	1571	C5-C6 (33%), N7-C5 (17%), C6-N1 (8%)
	1509 (m)	1522	C4-N3=C2 (13%), C8=N7 (12%), C2=N3 (10%), N1-C2 (9%)
1456 (s)	1454 (s)	1462	N1-C2-H (22%), N3=C2-H (11%), C5=C4 (11%), C2=N3 (8%)
1435 (m, sh)	1434 (m, sh)	1437	C4-N9 (29%), C2=N3 (14%), N9-C8 (8%), N3-C4 (8%)
	1372 (w)	1374	N9-C8 (22%), C2=N3 (11%), H-N9-C8 (10%), N1-C2 (9%), N3-C4 (8%), H-N9-C4 (8%)
1345 (w)	1338 (m)	1323	N3=C2-H (35%), N1-C2-H (25%), C5=C4 (9%)
1283 (sh)	1286 (w)	1258	C6-N1-H (40%), C2-N1-H (27%), C6=O (15%)
1254 (m)	1253 (m, br)	1241	H-N9-C8 (37%), H-N9-C4 (28%), C8=N7 (9%)
	1147 (s)	1160	C6-N1 (28%), N7-C5 (18%), N1-C6=O (8%)
1106 (w)	1102 (m)	1090	N1-C2 (15%), C6=O (15%), N3-C4 (10%), N9-C8 (8%)
940 (w, br)	950 (m, br)	968	N7=C8-D (24%), N9-C8 (12%), N9-C8-D (12%), N1-C2 (10%)
	930 (sh)	914	N1-C2 (14%), C4-N3=C2 (8%), N7=C8-D (8%), C2=N3 (8%), C4-N9-C8 (8%)
		855	N9-C8-D (40%), N7=C8-D (24%)
719 (m)	716 (m, br)	691	N3-C4 (10%), N1-C2 (9%), N1-C6-C5 (8%)
621 (w)	626 (m)	617	C6-N1 (12%), C8=N7-C5 (9%), N7-C5=C4 (9%), C4-N9 (8%)
546 (w)	550 (m)	560	N7-C5 (22%), C6-N1 (15%), C6-C5=C4 (9%), N7-C5-C6 (9%), C5-C6=O (8%)
	529 (sh)	517	N3-C4 (17%), C4-N9 (15%), N3-C4-N9 (15%), N1-C6=O (11%)
		310	C5-C6 (26%), C5-C6=O (24%), N1-C6=O (18%)

Table 4. Same as Table 2, but for H-d2 (N1-, N9-deuterated derivative of hypoxanthine). See also Fig. 3

RRS 257 nm	RRS 281 nm	Calc.	Assignments (PED)
		1707	C6=O (38%), C6-N1 (8%)
1674 (m, br)	1673 (m, br)	1671	N3-C4 (23%), C6=O (22%), C2=N3 (14%), C5-C6 (11%)
1576 (s)	1576 (sh)	1584	C8=N7 (20%), C6-N1 (7%)
1548 (s)	1554 (vs)	1572	C5-C6 (32%), N7-C5 (16%)
1498 (s)	1498 (s)	1518	C4-N3=C2 (14%), N1-C2 (12%), C8=N7 (11%), C2=N3 (10%)
		1447	N1-C2-H (27%), N3=C2-H (14%), C2=N3 (14%), C5=C4 (10%)
1429 (m)	1430 (w)	1435	C4-N9 (29%), N9-C8 (18%)
1359 (s)	1357 (s)	1385	N9-C8 (18%), C2=N3 (15%), N1-C2 (12%), N3-C4 (11%), N7=C8-H (9%)
1342 (s, h)	1336 (m, sh)	1321	N3=C2-H (34%), N1-C2-H (24%), C5=C4 (10%)
1252 (w)	1260 (w)	1246	N7=C8-H (41%), N9-C8-H (38%)
		1143	C6-N1 (27%), N7-C5 (21%), N1-C6=O (8%), N1-C2 (8%)
1098 (m)	1097 (m)	1103	C6=O (24%), N1-C2 (12%), N3=C2-H (8%), N1-C2-H (8%)
	970 (m, br)	1015	C6-N1-D (25%), C2-N1-D (10%), C4-N9 (8%)
962 (m)		962	D-N9-C8 (38%), D-N9-C4 (21%), N9-C8 (11%)
	888 (w)	881	N1-C2 (12%), D-N9-C4 (9%), N9-C8-H (9%), C2-N1-D (8%), C8=N7-C5 (8%)
		828	D-N9-C4 (17%), C2-N1-D (13%), N1-C2 (13%), C6-N1-D (10%)
716 (m)	717 (w)	683	C2-N1-D (12%), N3-C4 (11%), C2-N1-C6 (8%)
610 (m)	608 (m)	602	C6-N1 (14%), C4-N9 (8%), C5-C6 (8%), N7-C5=C4 (8%), C8=N7-C5 (8%)
548 (w)		554	N7-C5 (23%), C6-N1 (13%), C6-C5=C4 (9%), N7-C5-C6 (8%)
	530 (vw)	508	N3-C4-N9 (15%), C4-N9 (15%), N3-C4 (13%), N1-C6=O (12%)
		312	C5-C6 (26%), C5-C6=O (25%), N1-C6=O (18%)

ments, three spectral regions including different types of vibrational modes can be distinguished, which we now want to discuss, at least for the major intensity bands observed experimentally. This will give us the opportunity to underline the specificity of hypoxanthine vibrational motions, as compared to other biological purines such as adenine and guanine.

A. 1750–1500 cm^{-1} spectral region

This is the region of almost pure bond stretching motions, for ring and exocyclic C6=O bonds. Five vibrational modes are calculated in this region (Table 2). A broad and rather weak Raman band observed around 1690 cm^{-1} is assigned here to two vibrational modes calculated at 1720 and 1682 cm^{-1}, respectively. Both of them arise from coupling of the carbonyl bond to the pyrimidine ring bonds stretchings (Fig. 4). These modes are sensitive to N1-deuteration (Fig. 3, Tables 4–5). It is worth mentioning that the IR spectrum of a polycrystalline powder of hypoxanthine shows a very large and composite band in the 1720–1680 cm^{-1} region (Majoube 1993), which dominates the whole IR spectrum. In addition, a peak at ca. 1720 cm^{-1} has been observed in the Raman spectra of

Table 5. Same as Table 2, but for H-d3 (C8-, N1-, N9-deuterated derivative of hypoxanthine). See also Fig. 3

RRS 257 nm	RRS 281 nm	Calc.	Assignments (PED)
		1706	C6=O (38%), C6-N1 (8%)
1674 (s, br)		1671	C6=O (23%), N3-C4 (22%), C2=N3 (14%), C5-C6 (11%)
1582 (m)	1582 (m, sh)	1576	C5-C6 (18%), C8=N7 (16%), C6-N1 (13%), C2=N3 (9%), N7-C5 (9%), N1-C2 (8%)
1551 (s)	1544 (vs)	1567	C8=N7 (25%), C5-C6 (17%), N7-C5 (9%), C6=O (8%)
1484 (s, br, doublet)	1486 (s, br, doublet)	1511	C8=N7 (16%), C4-N3=C2 (13%), N1-C2 (10%), C6=O (10%), C2=N3 (8%)
		1447	N1-C2-H (27%), N3=C2-H (15%), C2=N3 (13%), C5=C4 (11%)
1419 (m)	1415 (m)	1424	C4-N9 (33%), C2=N3 (15%), N3-C4 (9%), N1-C2 (8%)
1351 (s, br)	1366 (m)	1351	N9-C8 (33%), N1-C2 (8%)
	1334 (m)	1321	N3=C2-H (34%), N1-C2-H (23%), C5=C4 (10%)
	1152 (w)	1156	C6-N1 (29%), N7-C5 (23%), N1-C6=O (8%)
1103 (m)	1096 (m)	1105	C6=O (24%), N1-C2 (13%), N3=C2-H (8%)
		1022	C6-N1-D (15%), D-N9-C8 (13%), C4-N9 (9%), C8=N7 (9%)
971 (w)	984 (w)	984	D-N9-C8 (19%), D-N9-C4 (16%), N7=C8-D (16%), C6-N1-D (14%), N9-C8-D (12%), C2-N1-D (8%)
946 (w)	945 (w)	942	N9-C8 (19%), N7=C8-D (17%), D-N9-C8 (9%), C8=N7-C5 (8%), N9-C8=N7 (8%)
		843	N1-C2 (21%), C2-N1-D (17%), C6-N1-D (13%), N7=C8-D (11%), N9-C8-D (9%)
		808	N9-C8-D (26%), D-N9-C4 (20%), N7=C8-D (13%), D-N9-C8 (12%)
716 (w)	712 (w)	680	C2-N1-D (12%), N3-C4 (10%), C2-N1-C6 (8%)
612 (m)	608 (m)	601	C6-N1 (14%), C8=N7-C5 (8%), C5-C6 (8%), N7-C5=C4 (8%), C4-N9 (8%)
552 (w)	541 (w)	549	N7-C5 (24%), C6-N1 (12%), C6-C5=C4 (9%)
		503	C4-N9 (16%), N3-C4-N9 (15%), N3-C4 (13%), N1-C6=O (12%)
		309	C5-C6 (26%), C5-C6=O (24%), N1-C6=O (18%)

structured poly(rI) (Brown et al. 1972; Chou et al. 1977), i.e. in homopolymer triple and quadruple chains involving hypoxanthine residues. This has been interpreted in terms of stretching motions of carbonyls involved in interbase H bonding in ordered structures: this carbonyl mode shifts to 1675 cm^{-1} in disordered poly(rI) in D_2O solution (Chou et al. 1977).

The 257 nm RRS spectrum yields a rather broad band at 1594 cm^{-1}, while the 281 nm spectrum shows an intense band at 1580 cm^{-1} (with a broadening in the high frequency side around 1595 cm^{-1}). The former corresponds mainly to an imidazole ring vibration, while the latter is assigned to a combination of imidazole and pyrimidine ring stretching motions (see Fig. 4). This is one of the most striking differences between guanine and hypoxanthine vibrational motions estimated in our calculations on these two molecules. For example, let us focus on the important C8=N7 (42%) stretching contribution of hypoxanthine to the mode calculated here at 1606 cm^{-1} (but also 8% contribution to the calculated 1531 cm^{-1} mode). An equivalent PED contribution of C8=N7 vibration has been calculated in the 1490 cm^{-1} region for guanine (22% at 1491 cm^{-1} and 20% at 1480 cm^{-1}), and in the 1475 cm^{-1} region (30%) for C8-deuterated guanine (Dhaouadi et al. 1993b). Ab initio calculations also predicted that C8=N7 stretching vibration of guanine is around 1480 cm^{-1} (Nishimura et al. 1985). On the other hand, as concerns this 1480 cm^{-1} mode of guanine it is worthwhile to recall that *i)* N2–C2 stretching motion also significantly contributes to it (Dhaouadi et al. 1993b), and *ii)* this band is strongly affected when DNA undergoes a specific interaction with drugs, such as actinomycin D, through the 2-amino group of guanine (Chinsky and Turpin 1978). This illustrated well the important role of an amino group in the C2 position for modulating the vibrational energy of another group (e.g. C8=N7) located far away from it in the same purine molecule. Consequently, it is understandable that the C8=N7 stretching energy can be unexpectedly large in a purine base where there is no 2-amino group, such as hypoxanthine. In addition, it is also consistent and remarkable that the C8=N7 PED contributions are progressively displaced towards lower wavenumber bands in proportion to progressive deuteration of the hypoxanthine molecule, although remaining above 1500 cm^{-1} (see Tables 2 to 5).

In the mode at 1516 cm^{-1} (calculated at 1531 cm^{-1}) which is more intense under 281 nm excitation, both rings contribute, mainly through motions of C2, N3, C4, N9 and C8 atoms, i.e. the lower part of the molecule (almost 50% of total PED, see Table 2 and Fig. 4). There is no equivalent of this extended motion in guanine (or in adenine), in the same wavenumber region. This Raman band is highly sensitive to C8- and/or N-deuterations (Fig. 3, Tables 3–5). It shifts to 1509 cm^{-1} on C8 deuteration (H-d1); on N-deuteration (H-d2 species) it gives rise to an intense Raman band at 1498 cm^{-1} in the RRS spectra obtained with both excitation wavelengths, and further downshifts to 1486 cm^{-1} in H-d3 spectra. The corresponding calculated frequency consistently follows parallel downshifts.

B. 1500–800 cm^{-1} spectral region

In this region vibrational modes mainly involve ring bond-stretching motions highly coupled with exocyclic C–H and N–H angular bendings: it is the most difficult to interpret, since owing to these couplings, a simple deuterium substitution at a single site will greatly affect the

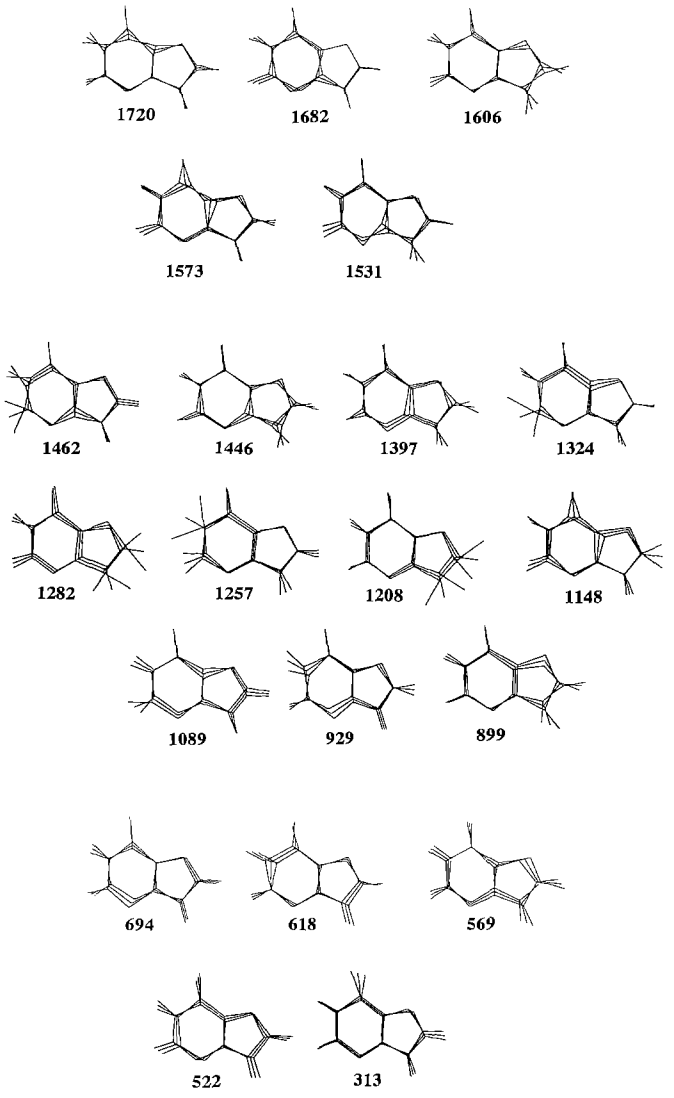

Fig. 4. Graphical representation of the calculated in-plane vibrational modes of hypoxanthine in the spectral region below 1800 cm^{-1}. The assignment of these modes in terms of internal coordinates is reported in Table 2

vibrational wavenumbers and the PED over all molecular motions (and bands). Eleven vibrational modes are calculated in this spectral region.

The most striking experimental spectra change in this region on deuteration is that the group of eleven lines observed experimentally in the 257 and 281 nm spectra of the native species is completely perturbed on C8 deuteration, and then gradually transforms on further deuteration into a large intensity doublet in the 1330–1360 cm^{-1} region and four medium/weak intensity bands around 950, 1100 and 1420 cm^{-1}. The group of three bands ranging from 1140 to 1286 cm^{-1} gradually changes and vanishes in going from the native species to H-d3. Simultaneously, new bands appearing above 1480 cm^{-1} are due to downshifts of modes from the previous group of pure ring stretching motions (see above).

The strong band observed at 1460 cm^{-1} for native species and 1456 cm^{-1} for H-d1, mainly assigned here to C2–H bending and pyrimidine double bond stretching motions, completely vanishes on N1, N9 deuteration (H-d2 and H-d3, Fig. 3). Similar behaviour has been observed for the same 1464 cm^{-1} band of poly(rI), although it was assigned to the cis Amide II group of hypoxanthine (Brown et al. 1972): it completely vanished when poly(rI) was in D_2O solution, and was thought to shift to 1335 cm^{-1}. Here the assignment is different, since we estimate only a 6% PED contribution on C6–N1–H bending motions for this band; however, the experimental observation is quite similar in both cases.

N9–C stretchings coupled with N9–H bending motions are responsible for the band observed around 1435 cm^{-1} (H and H-d1), which shifts towards 1430 and 1420 cm^{-1} in H-d2 and H-d3 spectra. The building of the strong doublet around 1340–1360 cm^{-1} on progressive deuteration is mainly due to the gradual downshift of the 1395 cm^{-1} band observed in H spectra (C2–N1, C2=N3 and C8–N7 stretchings, more or less coupled with H bendings), then constituting the higher component of the doublet. The lower component of the doublet mainly corresponds to C2–H bending coupled with C4=C5 stretching motions, which are essentially not affected by deuteration.

Now comes the problem of the interpretation of the drastic spectral changes observed in the 1300–800 cm^{-1} region on progressive deuteration: a careful examination of the PED values listed in Tables 2 to 5 helps a lot. The experiments show three modes at 1286, 1278 and ca. 1220 cm^{-1} in the native species spectra: the PED assigns to strongly coupled C8–H and N9–H bending motions two modes calculated at 1282 and 1208 cm^{-1}, and to N1–H bending coupled with C6=O stretching motions a mode calculated at 1257 cm^{-1} (see also Fig. 4). Deuteration at C8 on one hand (H-d1), at N1 and N9 on the other hand (H-d2), result in a complete decoupling of these bending motions. In the first case, C8–D bending motions shift down to 968 cm^{-1} (950 cm^{-1} observed), in the second case N1–D, N9–D and N9, N1–D bending motions shift down to calculated 1015, 962 and 881 cm^{-1}, respectively, and observed at 970, 962 and 888 cm^{-1}. Finally, deuteration at C8, N1 and N9 positions (H-d3 species) leads to an efficient recoupling of all C–H and N–H bending modes, calculated and observed at 984 cm^{-1}, and to C8–D bendings coupled with ring angular deformations around the C8 position, calculated at 942 cm^{-1} and observed at 945 cm^{-1}. Consequently, in all spectra of Fig. 3, vibrational modes can be observed in the ca. 950 cm^{-1} region, but their assignments totally differ from each other as a function of the deuteration scheme.

A last comment concerns a band appearing at ca. 1100 cm^{-1} in all spectra of Fig. 3. This mode is in all cases assigned to a global ring stretching motion of the whole molecule, with an important C6=O contribution, and is calculated at the same wavenumber. It is not sensitive (wavenumber and intensity) to deuteration.

C. Below 800 cm^{-1}

The present calculations lead to five vibrational modes in this region. As in the case of other purine bases, these

modes mainly involve intracyclic angular deformations coupled with bond-stretch motions: they are only weakly affected by deuteration. They generally give rise to weak RRS bands. Among those, the presence here of two bands located at ca. 720 and 620 cm^{-1} (Fig. 3) should be noted: they are calculated at 694 and 618 cm^{-1}, respectively (Fig. 4 and Table 2). Both modes present strong ring breathing characters. On the basis of our previous work on purine bases, the guanine molecule yields two main breathing modes at 664 and 577 cm^{-1} (Dhaouadi et al. 1993 b), while adenine gives rise to two modes of the same type at 742 and 643 cm^{-1} (Dhaoudi et al. 1993 a), respectively. In off-resonance Raman spectra of nucleic acids, purine ring-breathing modes generally give rise to intense bands in this region, which are commonly used as conformational markers. Their importance for monitoring right-to-left-handed DNA conformational transitions has been previously discussed (Thamann et al. 1981; Ghomi et al. 1988).

V. Conclusion

In a series of recent investigations, we have analyzed the vibrational spectra of native and deuterated nucleic acids purine bases. Two powerful experimental techniques, i.e. NIS and RRS spectroscopies, were used in order to study as completely as possible the in-plane and out-of-plane vibrational modes of adenine (Dhaouadi et al. 1993 a) and guanine (Coulombeau et al. 1991; Dhaouadi et al. 1993 b). These experimental spectra also offered the opportunity to propose molecular empirical valence force fields, allowing the vibrational mode wavenumbers and spectral intensities to be simulated. In the present work and in a companion paper (Dhaouadi et al. 1994), we describe how the major purine base in-plane force fields can be transferred to minor bases (hypoxanthine and 2-aminoadenine) in order to analyze their vibrational modes provided by RRS spectra. The transferability is rather good, since only a limited number of off-diagonal terms of the force field had to be refined in order to obtain a satisfactory agreement between experimentally observed and calculated results.

Indeed, this constitutes the first step of the vibrational analysis of more complicated systems: the main aim of these investigations is to extend this approach to the case of nucleosides and nucleotides built with hypoxanthine and involved in nucleic acid chains, in order to study and to monitor the vibrational structural markers related to these fragments. One must mention that hypoxanthine seems to be a rather peculiar purine base, which yields quite different vibrational spectra as a function of the substituent located at the N9 position. Preliminary results with 9-methyl-hypoxanthine show quite different vibrational features from those of the native species (unpublished results). Work is now progress to assign the vibrational bands of inosine residues with different sugar pucker conformations.

Acknowledgements. This work has been supported by grants from the French Ministry of Research and Space (P.M.), EC TEMPUS Office (JEP 2327, A.T. and J.U.) and Slovak Ministry of Education and Science (Grant 1/990148/92). It is considered as a part of the requirements for the PhD thesis of Jozef Ulicny.

References

Brown KG, Kiser EJ, Peticolas WL (1972) The conformation of polycytidylic acid, polyguanylic acid, polyinosilic acid and their helical complexes in aqueous solutions from laser Raman spectroscopy. Biopolymers 11:1855–1869

Chinsky L, Turpin PY (1978) Ultraviolet resonance Raman study of DNA and of its interaction with actinomycin D. Nucl Acids Res 5:2969–2977

Chou CH, Thomas Jr GJ, Arnott S, Campbell Smith PJ (1977) Raman spectral studies of nucleic acids XVII. Conformational structures of polyinosilic acid. Nucl Acids Res 4:2407–2419

Coulombeau C, Dhaouadi Z, Ghomi M, Jobic H, Tomkinson J (1991) Vibrational analysis of guanine by neutron inelastic scattering. Eur Biophys J 19:323–326

Dhaouadi Z, Ghomi M, Austin JC, Girling RB, Hester RE, Mojzes P, Chinsky L, Turpin PY, Coulombeau C, Jobic H, Tomkinson J (1993 a) Vibrational motions of bases of Nucleic acids as revealed by neutron inelastic scattering and resonance Raman scattering. 1. Adenine and its deuterated species. J Phys Chem 97:1074–1084

Dhaouadi Z, Ghomi M, Coulombeau Ce, Coulombeau C, Jobic H, Mojzes P, Chinsky L, Turpin PY (1993 b) The molecular force field of guanine and its deuterated species as determined from neutron inelastic scattering and resonance Raman measurements. Eur Biophys J 22:225–236

Dhaouadi Z, Ghomi M, Mojzes P, Turpin PY, Chinsky L (1994) Ultraviolet resonance Raman spectra from aqueous solutions of 2-aminoadenine and its deuterated species. Eur Biophys J (in press)

Ghomi M, Letellier R, Taillandier E (1988) A critical review of nucleosidic vibration modes appearing in the 800–500 cm^{-1} spectral region based on a new harmonic dynamics calculations. Biopolymers 27:605–616

Gusoni M, Zerbi G (1968) Symmetry coordinates in molecular vibrations. J Mol Spectrosc 26:485–488

Livramento J, Thomas Jr GJ (1974) Detection of hydrogen-deuterium exchange in purines by laser-Raman spectroscopy. Adenine 5′-monophosphate and polyriboadenylic acid. J Am Chem Soc 96:6529–6531

Majoube M (1984) Vibrational spectra of guanine. A normal coordinate analysis. J Chim Phys (Paris) 81:303–315

Majoube M (1993) (private communication)

Medeiros GC, Thomas Jr GJ (1971) Raman studies of nucleic acids IV. Vibrational spectra and associative interactions of aqueous inosine derivatives. Biochim Biophys Acta 247:449–462

Mirau PA, Kearns DR (1984) Comparison of the conformation of poly(dI-dC) with poly(dI-dBr^{5}C) and the B and Z forms of poly(dG-dC). One- and two-dimensional NMR studies. Biochemistry 23:5439–5446

Miskovsky P, Chinsky L, Laigle A, Turpin PY (1989) The Z conformation of poly(dA-dT).poly(dA-dT) in solution as studied by ultraviolet resonance Raman spectroscopy. J Biomol Struct Dyn 7:623–637

Miskovsky P, Tomkova A, Chinsky L, Turpin PY (1993) Conformational transitions of poly (dI-dC) in aqueous solution as studied by ultraviolet resonance Raman spectroscopy. J Biomol Struct Dyn 11:655–669

Mitsui Y, Langridge R, Shortle BE, Cantor CR, Grant RC, Kodama M, Wells RD (1970) Physical and enzymatic studies of poly d(I-C).poly d(I-C), an unusual double-helical DNA. Nature 228:1166–1169

Nishimura Y, Tsuboi M, Kato S, Morokuma K (1985) In-plane vibrational modes of guanine from an ab initio MO calculation. Bull Chem Soc Jap 58:638–645

Sutherland JC, Griffin KP (1983) Vacuum ultraviolett circular dichroism of poly(dI-dC)$_2$: no evidence for a left-handed doublex helix. Biopolymers 22:1445–1448

Thamann TJ, Lord RC, Wang AHJ, Rich A (1981) The high salt form of poly(dG-dC).poly(dG-dC) is left-handed Z-DNA: Raman spectra of crystal and solutions. Nucl Acids Res 20:5443–5457

Thomas Jr GJ, Livramento J (1975) Kinetics of hydrogen-deuterium exchange in adenosine, 5′-monophosphate, adenosine 3′:5′ monophosphate and poly(riboadenylic acid) determined by laser-Raman spectroscopy. Biochemistry 14:5210–5218

Vorlickova M, Sagi J (1991) Transitions of poly(dI-dC), poly(dI-methyl^{5}dC) and poly(dI-bromo5dC) among and within the B-, Z-, A- and X-DNA families of conformations. Nucl Acids Res 19:2343–2347

Weidlich T, Lindsay SM, Peticolas WL, Thomas GA (1990) Low frequency Raman spectra of Z-DNA. J Biomol Struct Dyn 7:849–858

Wilson EB, Decius JC, Cross PC (1955) Molecular vibrations. McGraw Hill, New York